The potential of ZrO_2 catalysts for the dehydration of 2,3-butanediol into 3-buten-2-ol: Impact of synthesis method and operating conditions

Beruk A. Bekele[1], Jeroen Poissonnier[1], Joris W. Thybaut[1*]

[1]Laboratory for Chemical Technology, Ghent University, Technologiepark 125, B-9052, Ghent, Belgium

* Corresponding author email address: Joris.Thybaut@UGent.be.

Key words: hydrothermal ZrO_2 synthesis, 2,3-butanediol dehydration, biomass conversion, kinetics

Abstract

2,3-butanediol (2,3-BDO) dehydration towards 1,3-butadiene was investigated over commercial and in-house synthesized ZrO_2 catalysts in a Berty reactor at intrinsic kinetics conditions. The commercial and ZrO_2 catalysts prepared via precipitation (ZrO_2-PP) exhibited a higher selectivity towards the undesired methyl ethyl ketone which was attributed to a lack of sufficient acid-base concerted active sites. For ZrO_2-PP, this was attributed to its tetragonal crystal structure with weaker adsorption sites. Hydrothermal synthesis allowed producing ZrO_2 with a monoclinic crystal structure, with correspondingly more pronounced acidic and basic properties which could be further tuned via calcination. A maximal 3-buten-2-ol, i.e., the desired intermediate for further conversion into 1,3-butadiene, yield amounting to 38% (mol mol^{-1}) could be obtained under a N_2 flow at 300°C, a space time of 1130 kg s mol^{-1} and 2,3-BDO partial pressure of 0.16 bar over the hydrothermally synthesized catalyst.

1. Introduction

The vast majority of chemicals commercially available today can be traced back to crude oil. Aiming at minimizing the usage of fossil fuel resources, the demand and interest for sustainable production processes is growing rapidly. In this respect, biomass derived feedstocks show a great potential for the sustainable production of chemicals [1–4].

1,3-butadiene (BD) is among the most important monomers in the chemical industry as we know it today, with an annual production volume amounting to approximately 12 Mtonnes, and applications mainly in the production of styrene-butadiene-rubber (SBR), polybutadiene and acrylonitrile-butadiene-styrene (ABS) polymer products [5]. Currently BD is mostly obtained as a side product from naphtha steam cracking . The recent shift towards lighter feedstocks in steam cracking, stemming from process efficiency, economic viability and the shale gas revolution, is limiting the BD production [5,6]. As a consequence, the demand for alternative and, preferably more sustainable BD production processes has emerged. To date, various bio-based feedstocks have been investigated for BD production, with ethanol, 1-butanol and more recently butanediol isomers as the most notable ones [7–12].

Recent studies reporting a high yield of 2,3-butanediol (2,3-BDO) from sugar and xylose fermentation, imply a large potential for sustainable 2,3-BDO production [13–15]. In addition, 2,3-BDO can be produced from industrial waste gas by using nonpathogenic bacteria [16]. 2,3-BDO dehydration was first investigated by Winfield, who reported a combined selectivity of BD and 3-buten-2-ol (3B2OL) amounting to 80% (mol mol^{-1}) at 350°C over a ThO_2 catalyst. Given the radioactive nature of ThO_2, the further application potential of this catalyst was considered limited [17]. More recently, an assessment of the catalytic dehydration of 2,3-BDO over zeolites, modified zeolites, metal oxides and rare earth oxides showed that the first dehydration is the more

critical and challenging one [18]. Among the primary 2,3-BDO dehydration products, methyl ethyl ketone (MEK), 2-methyl propanal (2-MPAL), and 3B2OL were the main ones. 3B2OL was identified as the intermediate that is most easily further dehydrated to BD [18,19]. Hence, to ensure an overall optimal conversion into BD, the 3B2OL selectivity in the first dehydration is to be optimized.

Over ZSM-5 with Si/Al ratios of 38 and 360, the dehydration of 2,3-BDO resulted in near complete conversion at temperatures as low as 250°C and 300°C. The product spectrum on these zeolites mainly consisted of MEK (70% mol mol^{-1}) and 2-MPAL (25% mol mol^{-1}) [20]. Modification of the ZSM-5 catalyst with boric acid and P_2O_5 resulted in promotion of methyl shift reactions, allowing 2-MPAL formation already at 180°C [20,21]. The use of other zeolites such as H-BEA (Si/Al =75), dealuminated BEA and Zr modified BEA, resulted in large amounts of C8-C12 condensation products (63% mol mol^{-1}), next to MEK and 2-MPAL [22]. Cu/ZSM-5 bifunctional catalysts were also assessed for the hydrodeoxygenation of 2,3-BDO to butenes demonstrating that Cu metal sites are responsible for the (de)hydrogenation reactions [23]. Butenes was obtained by first forming 2-butanol and i-butanol and then further dehydration lead to formation of butenes.

Different types of alumina have been investigated by Zeng et al. [24] for the two-step dehydration of 2,3 BDO into 1,3 BD. The higher purity (SCFa) form of alumina resulted in a high selectivity towards MEK of 70% (mol mol^{-1}) at 300°C, which decreased with increasing temperature to a minimum of 57% (mol mol^{-1}) at 450°C, and correspondingly reaching a maximum BD selectivity of 28% (mol mol^{-1}) [24]. Addition of Na to this catalyst (SCFa-Na-7.6%) resulted in an increased formation of heavy components, exhibiting a selectivity up to 30% (mol mol^{-1}) while the selectivity towards a cracking product, acetone, amounted to 20% (mol mol^{-1}) [24]. Duan et al. investigated ZrO_2 and various rare earth oxides for the dehydration of butanediols and terminal diols [25]. Over

the ZrO_2 catalyst under N_2 diluent flow, a selectivity towards 3B2OL of 49% (mol mol^{-1}) was obtained at a 2,3-BDO conversion of 63% (mol mol^{-1}) at 325°C [26]. In addition, a CaO modified ZrO_2 variant was also exhibiting an improved 3B2OL selectivity of 76% (mol mol^{-1}) at 350°C at a 2,3-BDO conversion of 55% (mol mol^{-1}) [27]. Furthermore, Duan et al investigated several rare earth metal oxides for the dehydration of 2,3-BDO towards 3B2OL and found that a selectivity towards 3B2OL amounting to 85% (mol mol^{-1}) could be obtained over Sc_2O_3 at full 2,3-BDO conversion [28]. More recently, Sanyal et al investigated the selective dehydration of 2,3-BDO to 3B2OL over In_2O_3 synthesized in-house and obtained a maximum selectivity of 70% (mol mol^{-1}) at a 2,3-BDO conversion of 81% (mol mol^{-1}) [29].

The above results can be tentatively rationalized in terms of the acid base properties of the catalysts used. Catalysts such as γ-alumina and zeolites (ZSM-5, H-BEA, deAl BEA, Zr-BEA) are mainly selective towards dehydration products such as MEK and 2MPAL, while catalysts with metallic and basic properties lead to a higher selectivity towards 3-hydroxy-2-butanone (3H2BONE) and butenes [20,22,30–32]. Catalysts with weak basic and acidic functionality such as ThO_2 and Sc_2O_3 perform better in the selective dehydration of 2,3-BDO towards 3B2OL and BD. As ThO_2 is a radioactive material and Sc_2O_3 an expensive rare earth metal oxide, a more sustainable and economically viable catalyst, and correspondingly, process, is desirable. Therefore, the potential of such a catalyst, in terms of 'intrinsic' kinetics, usable in an industrial production process should be investigated in a wide range of conditions.

In this work, ZrO_2 is selected for a 2,3-BDO dehydration kinetics investigation because of its cooperative mild acidic as well as moderate basic properties [33]. In addition, to the best of our knowledge, an assessment of the potential of ZrO_2 catalysts including tuning of catalyst properties and detailed kinetic investigation for selective 3-buten-2-ol formation has not been performed yet.

2. Experimental

2.1. Catalyst materials and synthesis

In this work a commercial ZrO_2 (99.8%) catalyst was obtained from Alfa Aesar™. $ZrO(NO_3)_2.3H_2O$, urea (CH_4N_2O) and ammonium hydroxide $NH_4(OH)$ (28% NH_3 in H_2O) obtained from Sigma-Aldrich were used for the in-house synthesis of catalytic materials.

The ZrO_2 catalysts were synthesized in-house using a precipitation and a hydrothermal method. For the precipitation method, $ZrO(OH)_2$ (white precipitate) was first formed by the reaction of zirconyl oxynitrate hydrate ($ZrO(NO_3)_2.3H_2O$) and $NH_4(OH)$ at a pH of 10 followed by filtration, drying and finally calcination at 600°C or 800°C with a heating rate of 5°C/min. The calcination temperature was maintained for 3 h. The catalysts are denoted as ZrO_2_PP_600 and ZrO_2_PP_800 respectively.

For the hydrothermal method, a procedure reported by Li et al. was used to prepare ZrO_2 [34]. The zirconyl oxynitrate hydrate ($ZrO(NO_3)_2.3H_2O$) precursor was first dissolved in distilled water to obtain a solution of 0.5 M. Urea (CH_4N_2O) was then added to the solution and the reaction proceeded at 60°C for 2 h. The mixture was then treated in an autoclave for 20 h at a temperature of 160°C and autogenous pressure. Finally, the solution was filtered, washed and dried at 120°C in an oven overnight. Ultimately, the catalysts were calcined at 600°C or 800°C as was done for the precipitated catalysts. The catalysts are denoted as ZrO_2_HT_600 and ZrO_2_HT_800.

2.2. Catalyst characterization

2.2.1. Surface area measurement and porosity analysis

The surface area of the catalysts was investigated by N_2 adsorption at 77 K in a Micromeritics Tristar II apparatus. Each sample was degassed at 573 K for 3 h to remove any potentially adsorbed species on the surface. The specific surface area was determined using the Brunauer-Emmett-Teller (BET) method with p/p^o ranging from 0.01 and 0.99 [35,36]. The average pore size, total pore volume and pore size distribution were estimated from the desorption isotherm using the Barrett-Joyner-Halenda (BJH) method [35,37].

2.2.2. Acidity and basicity measurement

Acidity and basicity measurements were performed by temperature programmed desorption (TPD) with NH_3 and CO_2, respectively, as probe molecules in an AutoChem II 2920 (Micromeritics) instrument equipped with a thermal conductivity detector (TCD).

For acidity measurements the sample (± 0.2 g) was pretreated with high purity (99.999%) He at a flow rate of 25 ml/min during heating to 500°C with a heating rate of 10 °C/min. Next, the sample was kept at 500°C for 1 h and then cooled to 120°C. After pretreatment, the sample was saturated with NH_3 employing a flow of 4% (mol) NH_3 balanced in He at 120°C for 30 min. Subsequently, the physisorbed NH_3 was removed by flushing with pure He at 120°C for 1 h. The desorption analysis was then carried out by increasing the temperature to 800°C at a heating rate of 10 °C/min to make sure the non-occurrence of other species. The amount of ammonia desorbed is correlated to the peak area under the NH_3-TPD curve and quantified using a calibration curve for NH_3.

CO_2-TPD measurements were performed to determine the basicity of the catalysts. The sample (± 0.2 g) was pretreated with high purity He at a flow rate of 60 ml/min during heating to 600°C with a heating rate of 10 °C/min. Next, the sample was kept at 600°C for 1 h and then cooled to 120°C.

After pretreatment, the sample was saturated with CO_2 employing a flow of pure CO_2 at 100°C for 4 h. Subsequently, the physisorbed CO_2 was removed by flushing with pure He at 120°C for 1 h. The analysis was carried out by increasing the temperature to 900°C at a heating rate of 10°C/min. The amount of CO_2 desorbed is correlated to the area under the CO_2-TPD curve and quantified using a calibration curve for CO_2.

2.2.3. XRD analysis

The crystal structure of the catalysts was identified using powder X-ray diffraction (XRD). The analyses were performed using a Bruker D8-AXS Discover setup and a linear Vantec detector, and a CuKα X-ray source (λ = 1.54 Å) under continuous scanning mode. Data were analyzed from 2Θ angles of 20° to 80° in continuous scanning mode. Average crystallite sizes of ZrO_2 were calculated using the Scherrer equation [38]:

$$D = \frac{0.9 \cdot \lambda}{\beta \cdot Cos\ \theta}$$

Where θ is the Bragg angle, β is the full width at half maximum (FWHM) of the m-zirconia peak centered at 2Θ = 28.2° and t-zirconia centered at 2Θ = 30.2°

2.3. Catalytic test setup and analysis

The kinetic experiments were performed using a Berty reactor set up, a gas-solid continuous stirred tank reactor (CSTR) with complete internal mixing [39]. The reactor is essentially the same as used previously and full details can be found in a previous paper from our group [40]. 2 g of the catalyst mixed with the inert material, α-alumina for which the inertness has been verified a priori is loaded in the stationary catalyst basket. After closing, the reactor is heated up to the reaction temperature under a constant flow of nitrogen (5 NL/h). After reaching the reaction temperature, the reactor was flushed with a constant flow of nitrogen (10 NL/h) for 1 h to clean the surface of the catalyst

from adsorbed species. No H_2 was used in the experiments or pretreatment procedures, as the active phase is the metal oxide. The stirring of the reactor is set to 1500 rpm during reaction. 2,3-BDO is fed from a Knauer pump (p4.1S) at flow rates ranging from 0.01 ml/min to 0.2 ml/min. The 2,3-BDO is then mixed with N_2, vaporized in the evaporator and sent to the reactor inlet as a gas. A Thermo Scientific gas chromatograph (Trace 1310) equipped with a Flame Ionization Detector (FID) and Restek (Rtx-DHA-100) column is used for quantitative reaction mixture analysis. The method parameters used in the analysis are shown in Table 1. Methane was used as internal standard (IS) for quantification and mass balance verification based on an on-line GC analysis of the effluent. Additionally, the condensable products were collected for identification of the heavy components using an offline GC-MS analysis.

Table 1: Method parameters for GC analysis.

Injection	523 K, split flow: 400 ml/min
Analytical column	Restek, Rtx-DHA-100
	100 m x 0.25mm x ID, 0.5 µm
Carrier gas	He, constant pressure at 3.1 bar
Oven temperature	323 K (5 min) – 30 K/min – 523 K (10 min)
Detector	FID, 573 K

2.4. Intrinsic kinetics verification

The absence of potential heat and mass transfer limitation is verified using the relevant engineering criteria for the experiment with the most severe operating conditions. The absence of external mass transfer limitations is verified using the Carberry number [41]. The highest Carberry number obtained amounts to 10^{-7} which is five orders of magnitude below the limiting value of 0.05. The absence of internal mass transfer limitations was assessed using the Weisz-Prater criterion. The

highest value of Weisz modulus from all the components was 0.012 (2,3-BDO), being sufficiently below the limiting value of 0.08 [42]. The absence of external and internal heat transfer limitations was assessed via the Mears criterion and amounts to 0.01 K and 10^{-6} K respectively which are well below the limiting value of 0.15 K [43].

2.5. Definitions and data analysis

Firstly the GC calibration factors (CF) for each component were determined. The CF is determined experimentally by measuring the peak area of each component at different concentrations. When the relative peak area (RA) of a component is plotted at different concentrations (C), a linear plot is obtained with CF_i as slope.

$$CF_i = \frac{(C_i)}{(RA_i)}$$

The relative peak area and the calibration factors are then used to determine molar composition of the analyzed mixture.

$$y_i = \frac{(\mathrm{R}A_i) * CF_i}{\sum_{j=1}^{n}((\mathrm{R}A_j) * CF_j)}$$

The total flow is then calculated from the composition of CH_4 from the chromatogram and the known IS flow rate. The flow rate of all other components is ultimately calculated based on the determined total flow and composition.

$$F_i = y_i \cdot F_{tot} = y_i \cdot \frac{F_{IS}}{y_{IS}}$$

The carbon balance was verified to be closed within 15%, with a few exceptions where the carbon balance was closed within 20%, which is along the lines of what is reported in literature for this reaction [24]. For further processing, the flow rates were normalized to match the feed flow rate.

The conversion of 2,3-BDO (X_{BDO}) and the selectivity towards each product (S_i) were calculated as follows:

$$X_{BDO} = \frac{F_{BDO}^0 - F_{BDO}}{F_{BDO}^0} \cdot 100\% \qquad [\text{mol mol}^{-1}]$$

$$S_i = \frac{a_{Ci} \cdot F_i}{4 \cdot (F_{BDO}^0 - F_{BDO})} \cdot 100\% \qquad [\text{mol mol}^{-1}]$$

Where a_{Ci} represents the carbon number of component i, F_i its molar flow rate in the reactor effluent and F_{BDO}^0 the 2,3-BDO inlet flow rate. The factor four stems from the carbon number of 2,3-BDO.

Some coke formation on the inert material was visually observed after completion of the experimental campaign. However, this does not impact our observations and will, hence, not be investigated further in depth, as even under the most harsh conditions, i.e. a temperature of 375°C, no deactivation was observed within 4 weeks of operation.

3. Experimental results

3.1. Catalyst characterization

3.1.1. Surface area and porosity

The surface area, pore volume, and average pore size of the catalysts are characterized via N_2 adsorption. Calcination provokes a decrease in surface area, which is more pronounced at higher temperatures, as expected due to agglomeration for all types of catalysts, see Table 2. The pore volume of the commercial sample decreases from 0.24 cm^3/g to 0.11 cm^3/g while the average pore size of the remaining pores increases from 9.7 nm to 15.8 nm. Similar trends are observed for the catalysts synthesized using the hydrothermal and precipitation method when the calcination temperature is increased from 600°C to 800°C. As evident from Figure 1, the adsorption-desorption isotherm of the commercial and precipitated catalyst exhibited a type IV isotherm with a H3 hysteresis loop, which is defined by IUPAC as characteristic for a mesoporous material with non-rigid aggregates of plate-like particles [35]. The hydrothermally synthesized catalyst exhibited a type V isotherm with H2 hysteresis loop exhibiting a weaker adsorbate and adsorbent interaction and a narrow range of uniform mesopores [35,44]. A surface area of 38 m^2/g and 28 m^2/g was observed for the hydrothermally synthesized catalyst and the commercial one, respectively, after calcination at 800°C. On the other hand, the surface area amounting to 2.9 m^2/g for ZrO_2_PP_800 catalyst is within the measurement error, which indicates that the pore structure of the material might have entirely collapsed. Hence, this material was not considered for further testing.

Table 2: Specific surface area, pore volume, average pore size, acidity and basicity for the commercial and in-house synthesized catalysts.

[-] – undetermined

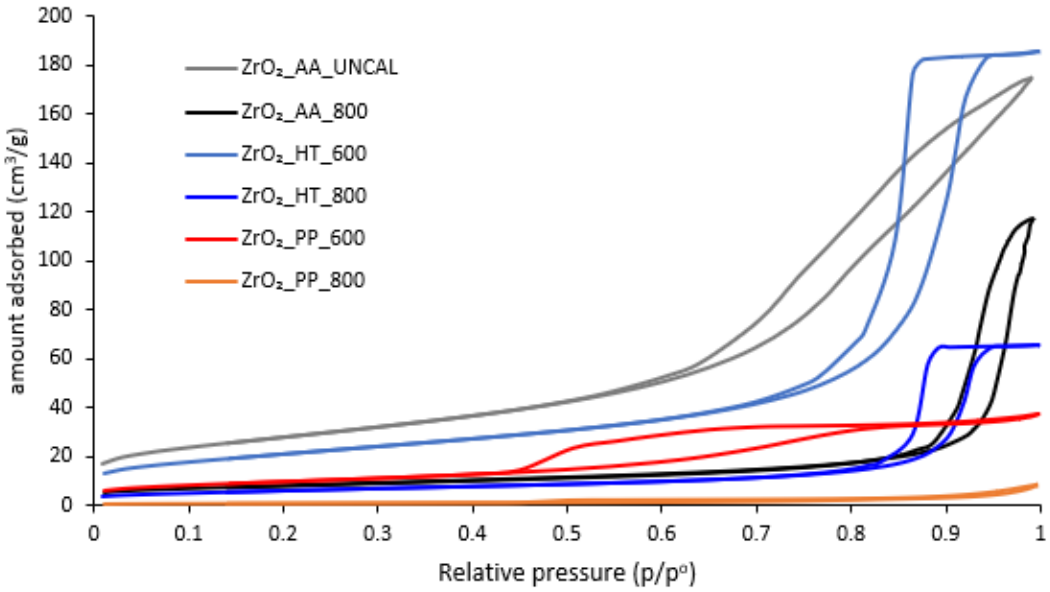

Figure 1: N_2 adsorption-desorption isotherms for the different ZrO_2 catalysts studied in this work.

Entry	Catalyst	BET Surface Area (m^2/g)	Pore volume (cm^3/g)	Average pore size (nm)	NH_3 uptake (mmol/g)	CO_2 uptake (mmol/g)
1	ZrO_2_AA_UNCAL	100	0.2	9.7	-	-
2	ZrO_2_AA_800	29	0.1	15.8	0.11	0.25
3	ZrO_2_HT_600	75	0.3	15.1	0.32	0.64
4	ZrO_2_HT_800	38	0.2	16.1	0.20	0.36
5	ZrO_2_PP_600	60	0.1	3.4	0.15	0.18
6	ZrO_2_PP_800	N. A	0.0	9.2	N. A	N. A

3.1.2. Acidity and basicity

In general, the acidity and basicity of the ZrO_2 catalysts decrease as the calcination temperature increases, see Figure 2 and Table 2. This can potentially be attributed to the loss of active sites via agglomeration from the calcination. Nevertheless, the hydrothermal catalyst still exhibits a clear acidity (≈0.2 mmol/g) and basicity (0.363 mmol/g) after calcination at 800°C, which is even higher than that of the precipitated catalyst calcined at 600°C, for which those values amount to 0.147 mmol/g and 0.181 mmol/g respectively. As the precipitated catalyst calcined at 800°C did not exhibit any significant BET surface area, the total acidity and basicity could not be determined i.e. no significant differentiation of the signal from the baseline could be observed. The ZrO_2_HT_600 catalyst contained the highest number of acid and basic sites, also exhibiting the strongest acidity and basicity of all investigated catalysts, albeit that overall the obtained values for acidity and basicity were mild. The ZrO_2_AA_800 catalyst contained a slightly lower number of acid sites than the ZrO_2_PP_600 catalyst, while the opposite is true for the number of basic sites.

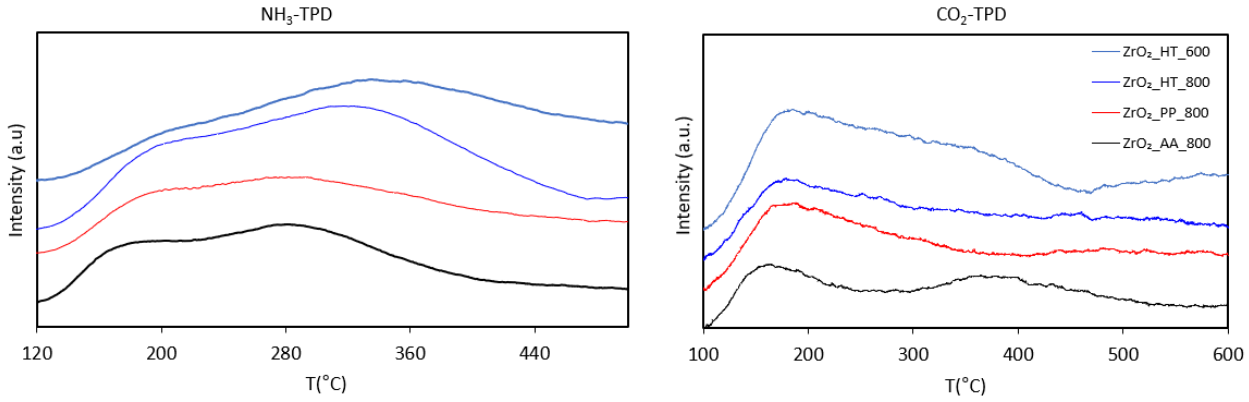

Figure 2: a. NH_3-TPD b. CO_2-TPD of ZrO_2_AA_800, ZrO_2_HT_600, ZrO_2_HT_800, and ZrO_2_PP_600 catalyst samples.

3.1.3. XRD Analysis

The XRD pattern of the three different types of samples is shown in Figure 3. The ZrO_2_AA_800 and ZrO_2_HT_800 catalyst exhibit very similar pattern with major peaks at 2Θ of 28.2 and 31.5, which are characteristic for monoclinic ZrO_2. The ZrO_2_PP_800 has a different pattern with a major peak at 2Θ of 30.2, characteristic for tetragonal ZrO_2.

Hence, a ZrO_2 catalyst with a monoclinic crystal structure is synthesized using the hydrothermal method, while a ZrO_2 catalyst with a tetragonal crystal structure is obtained using the precipitation method. The crystallite size of the three catalysts calculated using the Scherrer equation is presented in the Supplementary Information, Table S that of the tetragonal zirconia catalyst being significantly smaller than that of the monoclinic zirconia catalysts.

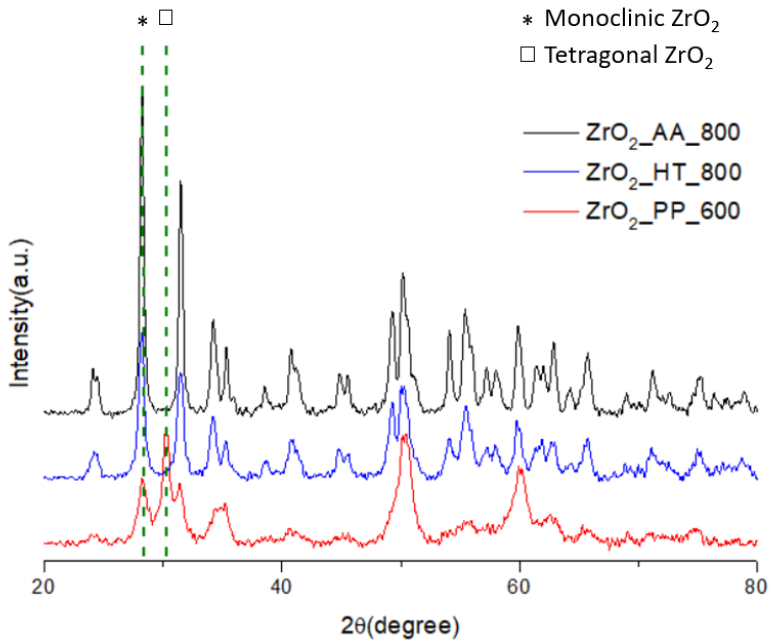

Figure 3: XRD pattern of different ZrO_2 samples.

3.2. Catalytic testing

3.2.1. Preliminary testing of the commercial catalyst

The initial 2,3-BDO dehydration experiments were conducted over the non-calcined commercial ZrO_2 catalyst. A 2,3-BDO conversion exceeding 80% (mol mol^{-1}) is obtained at a space time of 113 kg s mol^{-1} and reaction temperature of 325°C, see Table 3, entry 1. The selectivity towards 3B2OL amounted to only 10% (mol mol^{-1}), similar to that of the secondary product 2-butanol (2-BOL). The joint selectivity towards MEK and i-butanol (i-BOL) exceeds 60% (mol mol^{-1}). The selectivity towards 3-hydroxy-2-butanone (3H2BONE) remains below 15% (mol mol^{-1}). This is attributed to the presence of pronounced acidity and basicity and the high total number of active sites as was evident from the surface area in Table 2.

Next, the calcined version of the commercial catalyst was evaluated and the 2,3-BDO conversion and main products selectivity as a function of space time and 2,3-BDO inlet partial pressure are shown in Figure 4 a and b, respectively. The preliminary testing was performed at space times in the range of 14 to 113 kg s mol^{-1}. The conversion was limited to a maximum of 38% (mol mol^{-1}) compared to 80% (mol mol^{-1}) over the uncalcined catalyst at a similar space time of 113 kg s mol^{-1}, see Figure 4 a. This could be expected because of the decrease in the surface area due to agglomeration, see Table 2 in Section 3.1.1. The selectivity towards 3B2OL practically remained constant at 15% (mol mol^{-1}) irrespective of the space time, indicating that the second dehydration does not occur at these reaction conditions over this catalyst. The selectivity towards MEK exceeded 60% (mol mol^{-1}) at the lowest space time of 14 kg s mol^{-1} at the expense of the selectivity towards the other products, such as 2-MPAL and i-BOL which were not observed at any space time below 20 kg s mol^{-1}. The selectivity towards the dehydrogenation product, 3H2BONE is reduced from 20% (mol mol^{-1}) to 10% (mol mol^{-1}) as the space time increased from 14 to

113 kg s mol^{-1}. Thus, the dehydration reactions are favored as the space time and, hence, the 2,3-BDO conversion increases.

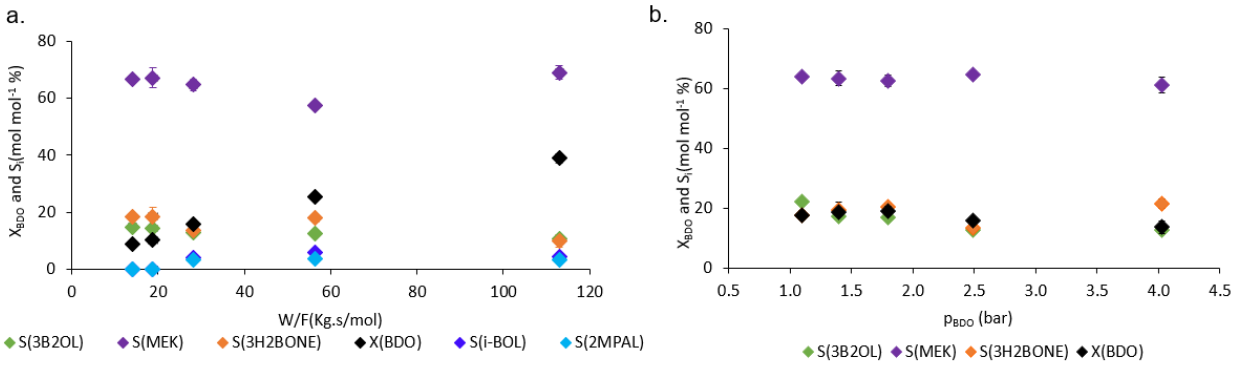

Figure 4: 2,3-BDO conversion and selectivity towards products over ZrO_2_AA_800 as a function of a. space time with the 2,3-BDO partial pressure amounting to 2.5 bar and b. 2,3-BDO inlet partial pressure at space time of 28 kg. s/mol at a temperature of 325°C and a total pressure of 10 bar.

The 2,3-BDO conversion does not change significantly as a function of its partial pressure as shown in Figure 4 b. The selectivity towards MEK is stable at 60% (mol mol^{-1}) and the selectivity towards both 3B2OL and 3H2BONE amounts to 18% (mol mol^{-1}). Almost no secondary products were formed, as also evident from Figure 4 a for the experiments performed at a space time of 28 kg s mol^{-1}. As the effect of the 2,3-BDO inlet partial pressure in the range from 1 to 4 bar is hardly significant, lower initial 2,3-BDO partial pressures (0.1–0.5 bar) were investigated in the following to also allow investigation at a higher space time.

The impact of temperature at iso-conversion of approximately 25% (mol mol^{-1}) for ZrO_2_AA_800 is presented in Table 3 at 350°C and 375°C. The selectivity towards MEK increased from 58% (mol mol^{-1}) to 66% (mol mol^{-1}) as the temperature was increased from 325°C to 350°C, while the 3H2BONE selectivity decreased from 18% (mol mol^{-1}) to 10% (mol mol^{-1}), see entries 2 and 3. The selectivity towards 3B2OL equaled 13% (mol mol^{-1}) at both temperatures.

Table 3: Catalytic testing for the dehydration of 2,3-BDO into 3B2OL over ZrO2 catalysts at a total pressure of 10 bar and inlet partial pressure of 2,3-BDO of 0.31 bar.

Entry	Catalyst	T(°C)	W/F (kg s mol^{-1})	X_{BDO} % (mol mol^{-1})	Selectivity% (mol mol^{-1})								
					3B2OL	MEK	3H2BONE	i-BOL	2-BOL	2-MPAL	DMP	BD	1-BENE
1[a]	ZrO_2_AA_UNCAL	325	113	81	10	41	14	24	9	2	0	1.5	0
2[a]	ZrO_2_AA_800	325	56.5	25	12	58	18	6	3	4	0	0	0
3[a]		350	28	25	13	66	10	5	4	3	0	0	0
4[a]		375	28	72	12	69	6	5	3	5	0	0	0
5	ZrO_2_PP_600	300	451.8	34	12	51	19	11	4	4	0	0	0
6		325	113	33	10	63	12	7	3	4	0	0	0
7		325	225.9	48	9	62	11	9	5	5	0	0	0
8		350	150.6	76	10	65	7	8	4	6	0	0	0
9		375	56.5	79	11	60	8	9	5	6	2	0	0
10	ZrO_2_HT_600	300	225.9	49	14	28	15	16	6	2	19	0	0
11		300	451.8	67	18	34	11	18	8	3	9	0	0
12		325	150.6	79	12	50	7	11	8	3	5	2	0
13	ZrO_2_HT_800	300	225.9	36	25	45	12	10	6	2	0	0	0
14		300	1130	67	26	35	10	13	7	3	7	0	0
15[b]		300	1130	89	42	33	5	13	8	0	0	0	0
16		325	113	38	19	53	13	6	7	2	0	0	0
17		350	1130	100	12	48	0	5	12	2	6	4	10
18		375	376.5	100	13	56	0	4	5	4	4	1	11

a – Inlet partial pressure of 2,3-BDO varied to 1.1 bar.

b – inlet partial pressure of 2,3-BDO varied to 0.09 bar.

3.2.2. Effect of crystal structure

The effect of the crystal structure of the catalyst is assessed using the precipitated catalyst, with a tetragonal structure and the hydrothermally synthesized one, with a monoclinic structure, both calcined at 600°C. In view of obtaining more dehydration products, a higher 2,3-BDO conversion was pursued and consequently the space time was varied between 113 and 1130 kg s mol^{-1}, i.e. a tenfold increase compared to the commercial catalyst testing. Full 2,3-BDO conversion is reached at a space time of 1130 kg s mol^{-1} over the tetragonal zirconia (ZrO_2_PP_600), see Figure 5. In addition, comparison of the progress of the reaction as a function of space time and temperature for the precipitated and hydrothermally synthesized catalyst, see Figure S5 of the Supplementary

Information, indicates that the activity of the different crystal structures is comparable however the different selectivity profiles are observed.

The 3B2OL selectivity amounts to only 10% (mol mol^{-1}), irrespective of the space time, which is a first indication for the better performance of monoclinic ZrO_2 catalysts in 2,3-BDO dehydration as the selectivity towards 3B2OL over the commercial ZrO_2 already amounted to 17% (mol mol^{-1}). The MEK selectivity decreased from 60% (mol mol^{-1}) to 40% (mol mol^{-1}) as the space time increases from 113 to 1130 kg s mol^{-1} because of its further conversion into secondary products. While the 3H2BONE selectivity at 113 kg s mol^{-1} still amounted to 15% (mol mol^{-1}) it was no longer observed at 1130 kg s mol^{-1} (3H2BONE selectivity of 0% (mol mol^{-1})). This behavior can be understood in terms of thermodynamic equilibrium being established between 3H2BONE and 2,3-BDO and, hence, no 3H2BONE is observed at full 2,3-BDO conversion, see also the experimentation over the different catalysts below. i-BOL and 2-BOL are the most prominent minor products over this catalyst. The selectivity towards i-BOL increases from 7% (mol mol^{-1}) at 113 kg s mol^{-1}, reaching 14% (mol mol^{-1}) at 376 kg s $mol^{-1}$and subsequently decreasing again to 11% (mol mol^{-1}) at 1130 kg s mol^{-1}. The 2-MPAL selectivity decreased slightly from 4% (mol mol^{-1}) to 2% (mol mol^{-1}) as the space time was increased from 113 to 1130 kg s mol^{-1}. At space times exceeding 225 kg s mol^{-1} BD was formed, its selectivity increasing to 6% (mol mol^{-1}) at a space time of 565 kg s mol^{-1} and remaining constant as the space time increased further to 1130 kg s mol^{-1}. The formation of two dimethylphenol (DMP) isomers, i.e. 2,5-DMP and 3,4-DMP, was also observed and confirmed via GC-MS analysis, see Figure S2 in the Supporting Information. At space times exceeding 282 kg s mol^{-1}, their combined selectivity increased from 3% (mol mol^{-1}) to 15% (mol mol^{-1}) at a space time of 1130 kg s mol^{-1}.

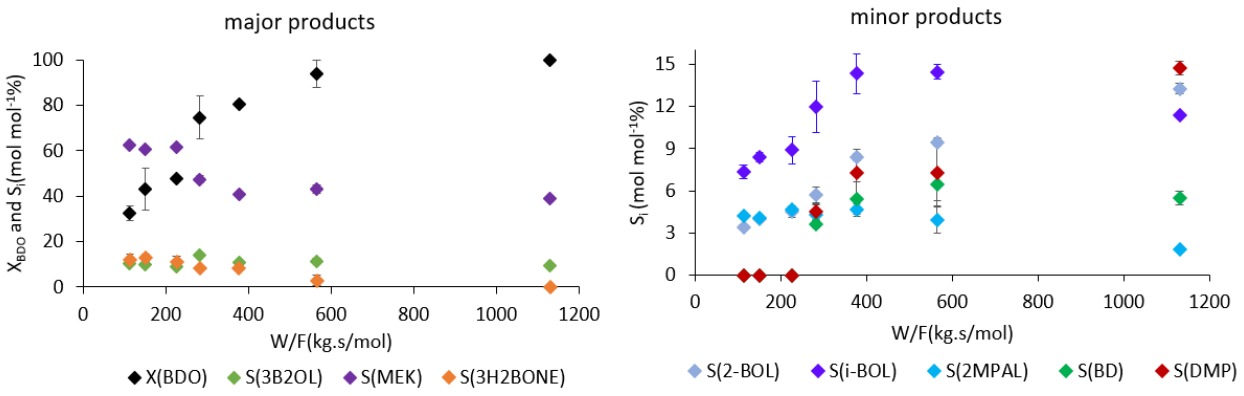

Figure 5: 2,3-BDO conversion and selectivity towards the products over ZrO_2_PP_600 as a function of space time at a temperature of 325°C and 2,3-BDO partial pressure of 0.31 bar and total pressure of 10 bar.

Figure 6 shows the 2,3-BDO conversion and product selectivity as a function of the space time over the monoclinic zirconia catalyst, ZrO_2_HT_600. The 3B2OL selectivity increased from 10% (mol mol^{-1}) to 20% (mol mol^{-1}) as the space time increased from 113 to 1130 kg s mol^{-1}. The MEK selectivity reaches a minimum of 40% (mol mol^{-1}) at 225 kg s mol-1 and amounts to maximally 52% (mol mol^{-1}) within the range 113 to 1130 kg s mol^{-1}. As was the case for the precipitated catalyst, 3H2BONE is no longer observed as 2,3-BDO is nearing full conversion with increasing space time, confirming the thermodynamic equilibrium. The selectivity towards i-BOL decreased only to a small extent from 12% (mol mol^{-1}) to 9% (mol mol^{-1}) while, similar to what was observed over the precipitated catalyst, the selectivity towards 2-BOL increased from 9 to 16% (mol mol^{-1}) as the space time was increased from 113 to 1130 kg s mol^{-1}. The 2-MPAL selectivity gradually decreased from 4% (mol mol^{-1}) to 2% (mol mol^{-1}), similar to what was observed over the precipitated catalyst, while BD was observed but its selectivity remained limited to 6% (mol mol^{-1}). In addition, the selectivity towards DMP decreased to zero at a space time of 1130 kg s mol^{-1} after exhibiting a maximal selectivity of 8% (mol mol^{-1}) at 211 kg s mol^{-1}, in contrast to 15% at a space time of 1130 kg s mol^{-1} over the precipitated catalyst.

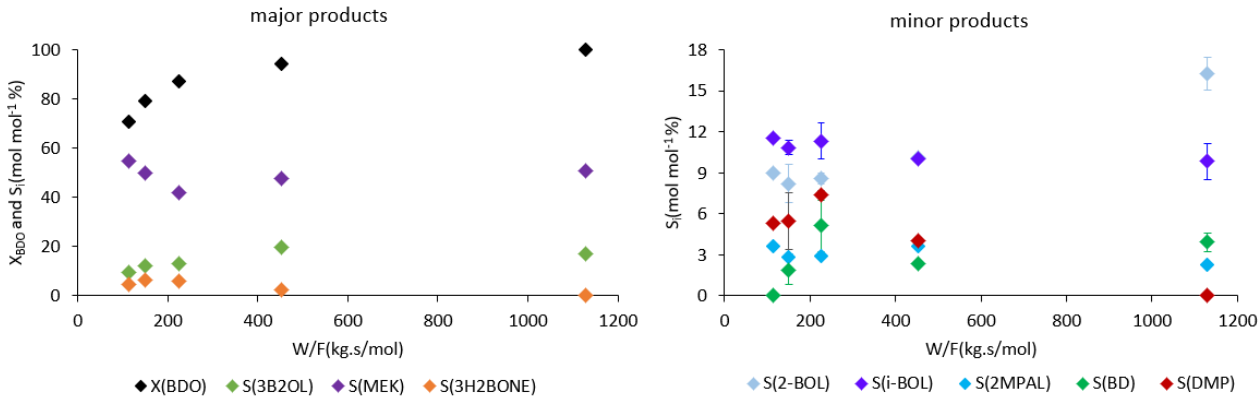

Figure 6: 2,3-BDO conversion and selectivity towards the products over ZrO_2_HT_600 as a function of space time at a temperature of 325°C and 2,3-BDO partial pressure of 0.31 bar.

The selectivity towards 3B2OL over ZrO_2_PP_600 and ZrO_2_HT_600 at a 2,3-BDO conversion of 48% (mol mol^{-1}), see entries 7 and 10 of Table 3, and 79% (mol mol^{-1}), see entries 9 and 12, is slightly higher over the hydrothermal catalyst, albeit that it remains below 14% (mol mol^{-1}). The precipitated catalyst resulted in a MEK selectivity exceeding 60% (mol mol^{-1}) whereas the hydrothermal catalyst gave a selectivity below 50% (mol mol^{-1}) at these conversion levels. Yet, DMP is formed with a selectivity up to 19% (mol mol^{-1}) over ZrO_2_HT_600, such that this catalyst is not the most optimal either for 3B2OL production.

3.2.3. Effect of calcination temperature

As evident from Table 2, a higher calcination temperature results in a decrease of the surface area, acidic and basic properties of the catalysts. The former is affecting the 2,3-BDO conversion, as seen in the preliminary testing of the commercial catalyst and Figure 6 and Figure 7 for the hydrothermally synthesized one. The less pronounced acidic and basic properties in the ZrO_2_HT_800 catalyst compared to the ZrO_2_HT_600 catalyst result in a 3B2OL selectivity increase of 5% (mol mol^{-1}) to 25% (mol mol^{-1}) at space times exceeding 225 kg s mol^{-1} and 10% (mol mol^{-1}) to 20% (mol mol^{-1}) at space times below 225 kg s mol^{-1}. More importantly, the

selectivity towards MEK reduced from 52% (mol mol^{-1}) at a space time of 113 kg s mol^{-1} to 37% (mol mol^{-1}) at the space time of 1130 kg s mol^{-1} for the hydrothermal catalyst calcined at 800°C while the catalyst calcined at 600°C did not exhibit such a decrease in MEK selectivity. In both cases, i-BOL is the secondary product exhibiting the highest selectivity except at a space time of 1130 kg s mol^{-1}, where the selectivity towards 2-BOL again exceeds the one towards i-BOL. While a maximum selectivity towards 2-BOL amounting to 16% (mol mol^{-1}) is reached at a space time of 1130 kg s mol^{-1} over ZrO_2_HT_600, the i-BOL selectivity is, correspondingly, minimized to 7% (mol mol^{-1}). Similarly, over the ZrO_2_HT_800 catalyst, the selectivity towards 2-BOL reaches a maximum of 14% (mol mol^{-1}) at a space time of 1130 kg s mol^{-1}, while the selectivity towards i-BOL is, correspondingly, reduced to 6% (mol mol^{-1}). Interestingly, at a 2,3-BDO iso-conversion of 86% (mol mol^{-1}), DMP exhibits a maximal selectivity of 8% (mol mol^{-1}) at a space time of 211 kg s mol^{-1} over ZrO_2_HT_600 while the maximal selectivity of 5.5% (mol mol^{-1}) over ZrO_2_HT_800 was sharper and observed already at a space time of 376 kg s mol^{-1}.

When comparing the 3B2OL selectivity at iso-2,3-BDO conversion of 67% (mol mol^{-1}) over the hydrothermally synthesized catalysts at 300°C, see Table 3 entries 11 and 14, an increase is observed from 18% (mol mol^{-1}) over catalyst calcined at 600°C to 26% (mol mol^{-1}) over the one calcined at 800°C. Over both catalysts the selectivity towards MEK was 35% (mol mol^{-1}). Thus, ZrO_2_HT_800 is a very promising catalyst with respect to 3B2OL formation and minimization of secondary products. The effect of other operating conditions is, hence, evaluated over this catalyst.

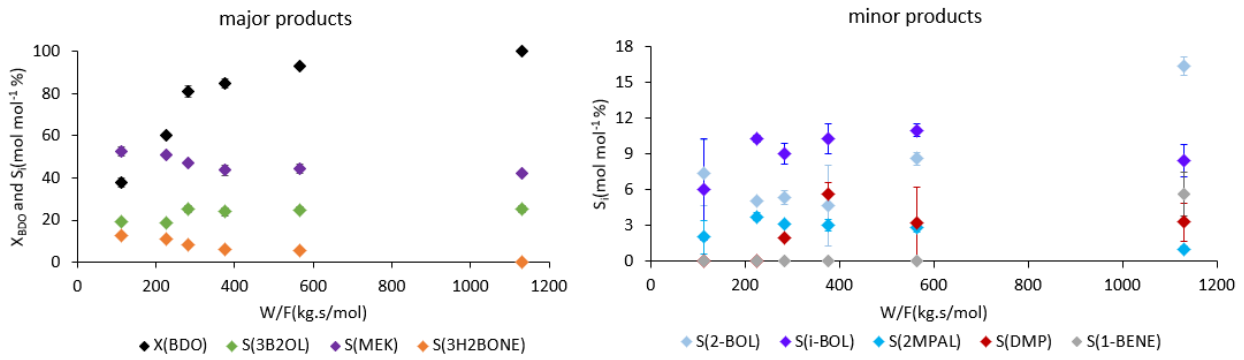

Figure 7: 2,3-BDO conversion and selectivity towards the products over ZrO_2_HT_800 as a function of space time at a temperature of 325°C and 2,3-BDO partial pressure of 0.31 bar and a total pressure of 10 bar.

3.2.4. Effect of reaction temperature on the hydrothermally synthesized catalyst

Figure 8 shows the effect of the reaction temperature on the 2,3-BDO conversion and product selectivity for the major products over ZrO_2_HT_800. The selectivity towards 3B2OL increases from 9% (mol mol^{-1}) to 31% (mol mol^{-1}) as the temperature was decreased from 375°C to 300°C at a space time of 565 kg s mol^{-1}. The corresponding selectivity towards MEK decreased from 54% (mol mol^{-1}) to 38% (mol mol^{-1}) as the temperature was increased from 300°C to 375°C. It is observed that the selectivity towards 3H2BONE also decreased from 11% (mol mol^{-1}) to 0% (mol mol^{-1}) as the temperature was increased 300°C to 375°C. At iso-conversion of 37% (mol mol^{-1}), see Table 3 (entries 13 and 16), the importance of operating at a lower temperature can be realized as the selectivity towards 3B2OL increased from 19% (mol mol^{-1}) to 25% (mol mol^{-1}) while the selectivity towards MEK decreased from 53% (mol mol^{-1}) to 45% (mol mol^{-1}) when the temperature was decreased from 325°C to 300°C. A more detailed description of the effect of reaction temperature on the minor product distribution is shown in the Supplementary Information, section S4.

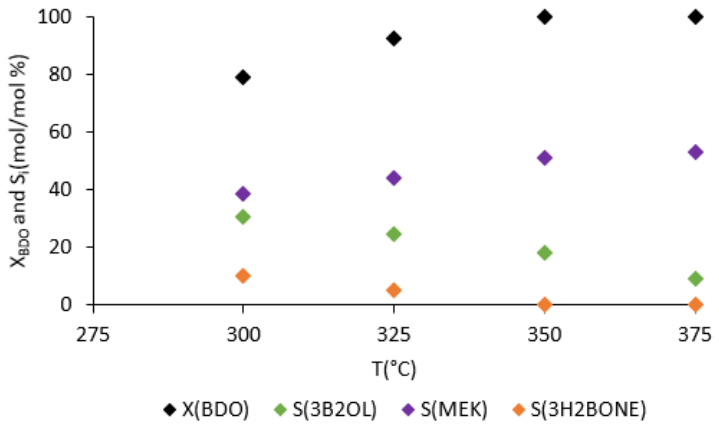

Figure 8: 2,3-BDO conversion and selectivity towards the major products as a function of temperature at space time of 565 kg.s mol-1 and 2,3-BDO partial pressure 0.31 bar.

3.2.5. Effect of 2,3-BDO partial pressure on the hydrothermally synthesized catalyst

The effect of the partial pressure of 2,3-BDO at the most promising conditions, i.e., at 300°C and 1130 kg s mol^{-1}, on its conversion and the product selectivity is shown in Figure 9. Interestingly, a maximum in 3B2OL selectivity amounting to 42% (mol mol^{-1}) is observed at a 2,3-BDO partial pressure of 0.16 bar and a 2,3-BDO conversion of 89% (mol mol^{-1}), while the MEK selectivity is, correspondingly, reduced to 34% (mol mol^{-1}), irrespective of the 2,3-BDO partial pressure. The selectivity towards 3H2BONE decreased from 11% (mol mol^{-1}) to 0% (mol mol^{-1}) as the partial pressure increased from 0.09 bar to 0.32 bar. Concluding, a selectivity of 42% (mol mol^{-1}) towards 3B2OL at a 2,3-BDO conversion of 89% (mol mol^{-1}) can be achieved with a hydrothermally synthesized ZrO_2 catalyst calcined at 800°C at 1130 kg s mol^{-1} at a temperature of 300°C and a total pressure of 10 bar, with the use of N_2 as diluent such that its inlet partial pressure amounts to 0.16 bar.

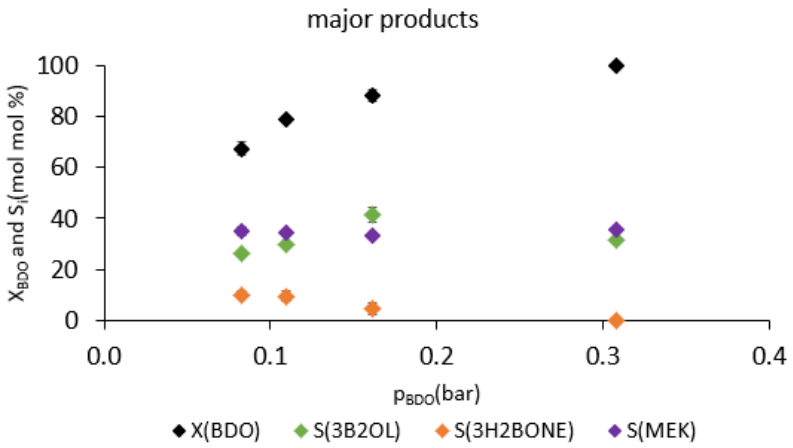

Figure 9: 2,3-BDO conversion and selectivity towards the major products over ZrO_2_HT_800 as a function of 2,3-BDO partial pressure at a temperature of 300°C and space time of 1130 kg s mol^{-1} and a total pressure of 10 bar.

4. Discussion

The catalyst preparation technique has a significant impact on the ZrO_2 catalyst properties. The hydrothermal synthesis method resulted in a monoclinic crystal structure with more pronounced acidity and basicity, while the precipitated one has a tetragonal crystal structure with acidic and basic sites of a lesser strength. This was evident from the desorption temperatures in NH_3-TPD and CO_2-TPD on the monoclinic catalyst exceeding those of the corresponding peaks for the tetragonal catalyst, see Figure S2 and S3 in the Supplementary Information. This is partly attributed to the potential of the monoclinic crystal structure to bare stronger adsorption sites than the tetragonal crystal structure as demonstrated by Jung et al. [45]. These authors also suggested that the crystal structure of zirconia affects the number and strength of the surface adsorption sites. In addition, the stronger adsorption sites are essential in establishing more interaction between the reacting species and the catalyst resulting in the formation of a higher amount of 3B2OL over the monoclinic ZrO_2 catalyst. The latter is even better illustrated by the results at space times exceeding 376 kg.s/mol; the 3B2OL selectivity over the monoclinic catalysts increased as function of space time as long as the operating temperature remained below 350°C, see Figure 7. Over the precipitated catalyst

calcined at 600°C, the 3B2OL selectivity remained below 15% (mol mol^{-1}) independent of the operating conditions because of its low number of acid-base concerted sites and weak adsorption sites resulting in weak interaction with the basic sites to activate the C-H bond, resulting in the formation of undesired secondary and tertiary products. Consequently, in terms of 3B2OL selectivity the hydrothermally synthesized catalyst outperformed the precipitated one thanks to the availability of relatively more acid-base concerted sites and strong adsorption characteristics. Thus, the active sites created on the surface of a monoclinic crystal structure ZrO_2 synthesized with the hydrothermal method are more suited for the formation of 3B2OL than a tetragonal crystal structure.

A selectivity towards MEK exceeding 60% (mol mol^{-1}) was obtained over the calcined commercial catalyst. 3H2BONE and 3B2OL dominated the remainder of the product spectrum at low space times while also some i-BOL and 2-BOL were formed at higher space times, albeit that their joint selectivity remained below 6% (mol mol^{-1}). This can be attributed to the monoclinic crystal structure of the commercial catalyst together with the remaining acidic and basic sites after calcination as evidenced in Table 2. Thus, the catalyst performance can be attributed to lower number of acid-base concerted sites which cannot be tuned via calcination.

The calcination temperature significantly affects the surface area, acidity and basicity of the catalyst for the hydrothermally synthesized catalyst, while the porous structure of the precipitated one collapsed into a dense structure by calcination at 800°C. Calcination at 800°C resulted in a more selective catalyst towards 3B2OL compared to the one calcined at 600°C, in agreement with the observations in literature [26]. This was attributed to weaker active sites characterized by cooperative acidic and basic sites as proposed by Tanabe [33], and evidenced from the NH_3 and CO_2 uptake values reported in Table 1. Even though the catalyst containing the stronger acidic and

basic sites, ZrO_2_HT_600, resulted in an improved selectivity towards 3B2OL compared to the precipitated one and a correspondingly decreased selectivity towards MEK, the catalyst is not suited as more DMP is formed, even at 300°C and 225 kg s mol^{-1} (Table 3 entry 10). Hence, the stronger active sites (both acid and base) in the ZrO_2_HT_600 are responsible for the formation of excessive undesired products, such as 2-BOL, i-BOL, DMP and coke rather than contributing to the 3B2OL formation, indicating the potential for 3B2OL selectivity enhancement by reducing the acidity and basicity of this catalyst.

The selectivity towards 3H2BONE over all investigated catalysts decreases as the 2,3-BDO conversion increases as a consequence of an increase in temperature and/or space time, which is attributed to the thermodynamic equilibrium with 2,3-BDO, in agreement with Duan et al and Zheng et al [31,32]. The amount of 2-MPAL produced is similar over all investigated catalysts, which indicates that the desorption of 2-MPAL from the ZrO_2 surface is difficult and, hence, i-BOL formation is most probable. BD was observed with a maximal selectivity of 6% (mol mol^{-1}) on the precipitated catalyst and both hydrothermally synthesized catalysts, pointing at the lack of stronger acidic sites to perform the second dehydration step. However, the presence of such stronger sites would compromise the desired selectivity in the first dehydration, rendering the direct, selective conversion of 2,3-BDO into BD extremely challenging,. The most pronounced DMP formation was observed over ZrO_2_PP_600 at 325°C and ZrO_2_HT_600 at 300°C implying that a minimum strength of basic sites is required for DMP formation and an even higher strength leads to degradation via coke formation at 1130 kg s mol^{-1} and 325°C over ZrO_2_HT_600.

The selectivity towards MEK especially increased with temperature, while lower temperature and higher space times are the key to achieve a high 3B2OL selectivity. However, also undesired products such as i-BOL, 1-BENE, and 2-BOL are formed to a more pronounced extent at higher

space times, such that the maximization of the 3B2OL selectivity cannot be achieved by merely maximizing the space time.

As shown earlier, the selectivity towards 3B2OL was significantly higher at a temperature as low as 300°C at high 2,3-BDO conversion, demonstrating the crucial effect of the temperature on the product spectrum, see also Figure 8. This result is in agreement with the work of Sayal et al. who reported an optimal temperature of 290°C for selective 3B2OL formation over the acid base concerted active site containing In_2O_3 catalyst [29]. From the mechanistic point of view, the relative ease of adsorption of the two OH groups of 2,3-BDO on the active sites, resulting in MEK formation, compared to adsorbing a H atom of the methyl group next to an adsorbed OH group to form 3B2OL could be related to the operating temperature, see Figure 10 [27]. Thus, we strongly suggest that, at a higher space time and a lower temperature there is a higher probability that 2,3-BDO molecules adsorb in a preferential manner, i.e. the surface interacts with a hydrogen from the methyl group, and vice versa. Adsorption in such a way is most probably required first before 3B2OL formation, which is probably enhanced by working at a high space time and a low reaction temperature and confirmed by the experimental observations in this work. In addition, the high space time or 2,3-BDO conversion ensures the minimization of 3H2BONE, in agreement with the thermodynamic equilibrium, thus making that ultimately more 2,3-BDO molecules have been able to undergo dehydration provided that 3H2BONE does not react further and the hydrogen remained available.

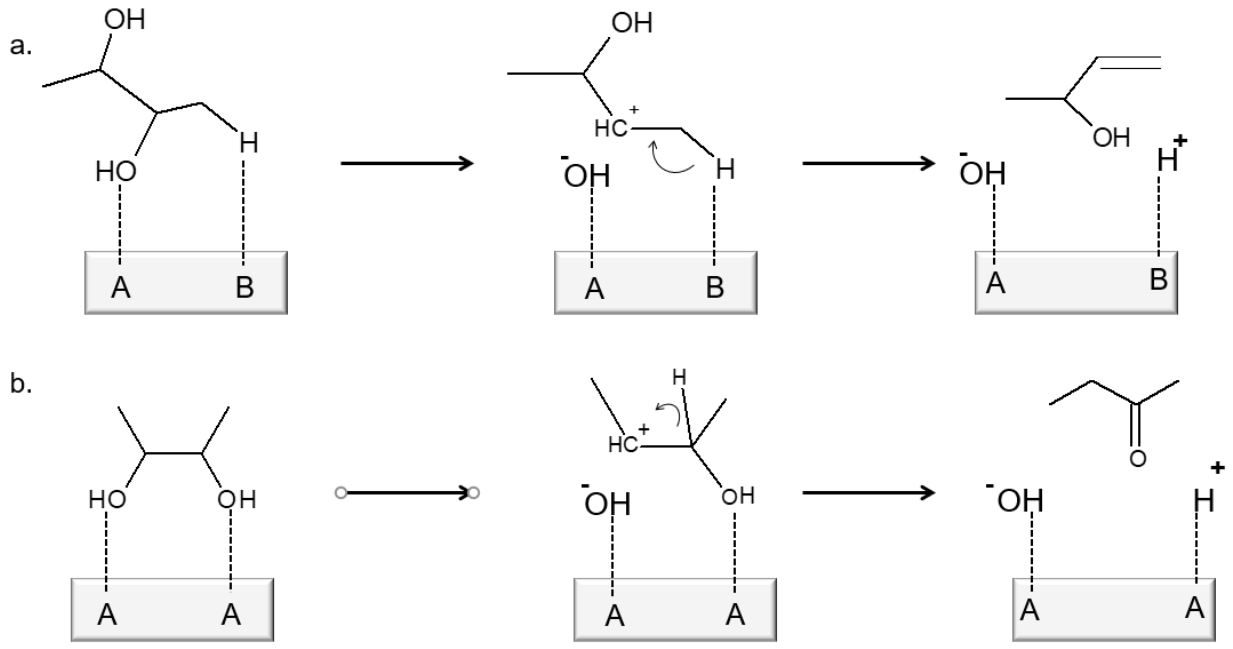

Figure 10: Adsorption and reaction mechanism for the formation of a. 3B2OL and b. MEK. Adapted and modified from Duan et al [27].

The dehydration of 2,3-BDO towards 3B2OL is a challenging reaction where both stronger or weaker acidity result in side products, MEK, 2-MPAL and 3H2BONE respectively [24,46–48]. These products lead to condensation to, e.g. DMP and even coking at more severe operating conditions [22,48]. On the other hand, on catalysts with weaker acid sites still produces excess MEK as illustrated for the precipitated catalyst and the calcined commercial catalyst. Thus the active sites for the reaction can be considered as only concerted acid-base sites and individual acid sites leads to formation of MEK. Consequently, the optimization of the challenging catalytic process requires action on both the side of the catalysts and operating conditions. The optimal conditions for the formation of 3B2OL on the ZrO_2 surface correspond to a space time of 1130 kg s mol^{-1}, a temperature of 300°C and partial pressure of 0.16 bar to achieve a selectivity of 42% (mol mol^{-1}) at conversion of 89% (mol mol^{-1}). This result is in line with previously reported results over a ZrO_2 type of catalyst at similar conditions, i.e., calcined at 800°C, using only N_2 as

a diluent (in a tubular reactor), where a 3B2OL selectivity amounting to 48.6% (mol mol^{-1}) was observed at a 2,3-BDO conversion of 62.5% (mol mol^{-1}) [26].

5. Reaction network elucidation

The reaction network of 2,3-BDO dehydration to 3B2OL can be unraveled from the intrinsic kinetic experiments in the Berty reactor over a wide span of operating conditions, covering the entire 2,3-BDO conversion level. The primary dehydration and dehydrogenation products 3B2OL, MEK, 2-MPAL and 3H2BONE were observed over the commercial catalyst during operation at a 2,3-BDO conversion limited to 25% (mol mol^{-1}). The primary nature of these products have been confirmed via a kinetic considerations, see Supplementary Information Section S5, Figure S6. The first step in the formation of MEK and 2MPAL can be related to the protonation of one of the adsorbed OH groups resulting in the formation of water (leaving group) which, in turn, results in the formation of a carbocation. MEK can then be formed by a facile hydride shift in the carbocation while a methyl shift allows the formation of 2-MPAL (pinacol rearrangement) [24]. Formation of 3B2OL occurs on electron acceptor-donor sites (acid-base concerted sites) via an E2 mechanism after adsorption of the carbonyl H and a β-H of the methyl group as shown in the reaction mechanism and the reaction network proposed in Figure 10 and Figure 11 respectively [26,27,49]. These sites can consist of either a cation (a Lewis acid) or a proton (Bronsted acid) bonded to a lattice oxygen atom [50]. Thus from the catalyst point of view, the product distribution depends on the relative amount of free acid sites to acid-base concerted sites. In contrast, 3H2BONE is formed from direct dehydrogenation of 2,3-BDO and can even further dehydrogenate to 2,3-butanedione, which was also observed in trace amounts in some of the experiments [31,32].

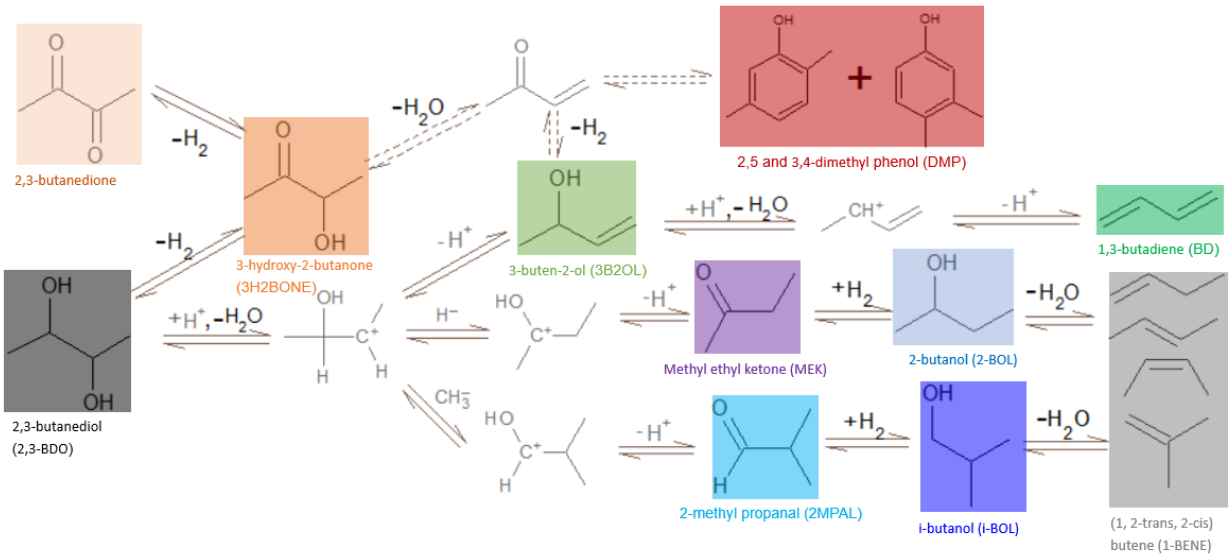

Figure 11: Proposed reaction network for 2,3-BDO dehydration over ZrO_2. The compounds shown in the colored boxes are experimentally observed, while intermediates are shown in grey. The dotted arrows show the proposed pathway for DMP formation (unconfirmed). 2,3-BDO is shown in the black box, 3H2BONE is shown in orange box, the DMP isomers are shown in dark red box, 3B2OL is shown in the light green box, BD is shown in the green box, MEK is shown in the purple box, 2MPAL is shown in the cyan box, i-BOL is shown in the blue box, 2-BOL is shown in the light blue box, and all butene isomers are shown in the grey box.

The formation of 2-BOL and i-BOL is the result of the hydrogenation of MEK and 2-MPAL, respectively, with H_2 generated from the formation of 3H2BONE and 2,3-butanedione. This was observed from the second order Del plot, see Supplementary Information Figure S6, in agreement with literature observations [51]. 2-BOL is formed in lower amounts than i-BOL, except at a space time of 1130 kg s mol^{-1}, which can be attributed to the reactive nature of the aldehyde functional group in 2-MPAL in contrast to its stable ketone counterpart in MEK.

Tertiary products were also observed during the dehydration of 2,3-BDO over the ZrO_2 catalysts. At temperatures exceeding 325°C, butenes were formed from the dehydration of 2-butanol and iso-butanol, as confirmed by feeding 2-butanol over the same catalyst, see Figure S2 of the Supporting Information. A maximum joint selectivity towards the different butene isomers of 13% (mol mol^{-1}) was observed at 375°C, while the produced 3H2BONE is practically completely converted to DMPs. In comparison, zeolite based types of catalysts allow the conversion of 2,3-BDO into

butenes already at 250°C [23,32], which is attributed to the stronger acid sites compared to the ZrO_2 catalysts. In this work, mainly 1-butene was observed among the butene isomers (i.e. ≈50%), which is attributed to the distinctive nature of ZrO_2 to produce alpha-olefins [52]. Dehydration of 2-butanol over the ZrO_2 catalyst resulted in the rather selective formation of 1-butene, and cis- and trans-2-butenes are observed as minor products, which has also been verified in this work. Iso-butene is not observed to a significant extent in most experiments except at 350°C and 375°C. As i-BOL is less reactive than 2-BOL and since the acid strength of the ZrO_2 active sites is not that high, this is not too surprising.

Two DMP isomers (2,5-DMP and 3,4-DMP) were observed in the product mixture. The formation of 2,5-DMP had been observed before for the dehydration of 2,3-BDO over ZrO_2 containing catalysts [53], yet the exact reaction path is still unclear. From our experiments it is strongly suspected that 3H2BONE is involved in the DMP formation. The DMP isomers could be obtained according to the Morita-Baylis-Hilman mechanism, as proposed by Salvapati [54], starting from methyl vinyl ketone. Methyl vinyl ketone can be obtained from the dehydration of 3H2BONE or the dehydrogenation of 3B2OL. The methyl vinyl ketone then undergoes a 1,4-addition to yield 3-methyleneheptane-2,6-dione. Next, a 1,6-aldol condensation and subsequent aromatization results in the formation of 2,5 and 3,4-DMP. Although both compounds are observed in the reaction mixture, the 3,4-DMP is found to a lesser extent than 2,5-DMP, most likely due to steric hindrance effects. This mechanism is also supported by the experimental results as 3,4-DMP is always formed in a lower amount than 2,5-DMP.

The formation of coke is initiated by species susceptible to coking such as 3H2BONE, 3B2OL, methyl vinyl ketone and 2,3-butadione. The H_2 produced during coking is used during the hydrogenation of MEK and 2-MPAL to 2-BOL and i-BOL respectively. This can explain why

catalysts with strong acidic and/or basic active sites are not selective towards 3B2OL but rather towards butenes and the small fraction of 3B2OL, being a coke susceptible species thus, leading to further reactions on those strong active sites.

6. Conclusions

The dehydration of 2,3-BDO in a Berty reactor operated at intrinsic kinetics conditions over a hydrothermally synthesized catalyst exhibited a 3B2OL yield up to 38% (mol mol^{-1}). A hydrothermal ZrO_2 catalyst calcined at 800°C outperforms the commercial ZrO_2 catalyst and the one synthesized using the precipitation method. This was attributed to the monoclinic crystal structure containing stronger adsorption sites for the commercial ZrO_2 and the hydrothermally synthesized one compared to tetragonal crystal structure of the one synthesized via the precipitation technique. Additionally, the hydrothermally synthesized catalyst contains more acid-base concerted sites than the one synthesized via the precipitation technique. Consequently, the hydrothermally synthesized ZrO_2 catalyst resulted in higher selectivity towards 3B2OL at appropriate conditions while the precipitated catalyst mainly resulted in the formation of MEK, almost irrespective of the operating conditions. Lower reaction temperatures (≈ 300°C) and higher space times (>376 kg s mol^{-1}) are crucial to ensure sufficient contact between the reacting species and the acid-base concerted sites such that a high selectivity of 42% (mol mol^{-1}) towards 3B2OL can be achieved. The ZrO_2 catalyst optimization as part of this work showed that stronger adsorption sites combined with only acid-base concerted active sites are required for a high selectivity towards 3B2OL. Within the context of BD production, the more pronounced acidity required for dehydration into 1,3-BD is detrimental for the primary product selectivity (3B2OL) in 2,3-BDO dehydration. Hence, the optimal ZrO_2 catalyst for 3B2OL formation is to be used in conjunction with a stronger acidic catalyst, such as γ-Al_2O_3, in a dual bed configuration for the production of green 1,3-butadiene.

7. Acknowledgments

This work was performed in the framework of the Catalisti cluster SBO project SPICY ("Sugar-based chemicals and Polymers through Innovative Chemocatalysis and engineered Yeast"), with the financial support of VLAIO (Flemish Agency for Innovation and Entrepreneurship) (HBC.2017.0597). We are grateful to the project coordinator for taking the lead in setting up the project.

8. References

[1] S.N. Naik, V. V. Goud, P.K. Rout, A.K. Dalai, Production of first and second generation biofuels: A comprehensive review, Renew. Sustain. Energy Rev. 14 (2010) 578–597. https://doi.org/10.1016/j.rser.2009.10.003.

[2] J.F. Jenck, F. Agterberg, M.J. Droescher, Products and processes for a sustainable chemical industry: A review of achievements and prospects, Green Chem. 6 (2004) 544–556. https://doi.org/10.1039/b406854h.

[3] A.M. Ruppert, K. Weinberg, R. Palkovits, Hydrogenolysis goes bio: From carbohydrates and sugar alcohols to platform chemicals, Angew. Chemie - Int. Ed. 51 (2012) 2564–2601. https://doi.org/10.1002/anie.201105125.

[4] T.W. Walker, A.H. Motagamwala, J.A. Dumesic, G.W. Huber, Fundamental catalytic challenges to design improved biomass conversion technologies, J. Catal. 369 (2019) 518–525. https://doi.org/10.1016/j.jcat.2018.11.028.

[5] W.C. White, Butadiene production process overview, Chem. Biol. Interact. 166 (2007) 10–14. https://doi.org/10.1016/j.cbi.2007.01.009.

[6] P.C.A. Bruijnincx, B.M. Weckhuysen, Shale gas revolution: An opportunity for the production of biobased chemicals?, Angew. Chemie - Int. Ed. 52 (2013) 11980–11987. https://doi.org/10.1002/anie.201305058.

[7] E. V Makshina, M. Dusselier, W. Janssens, J. Degrève, P. a Jacobs, B.F. Sels, Review of old chemistry and new catalytic advances in the on-purpose synthesis of butadiene., Chem. Soc. Rev. (2014). https://doi.org/10.1039/c4cs00105b.

[8] F. Jing, B. Katryniok, M. Araque, R. Wojcieszak, M. Capron, S. Paul, M. Daturi, J.M. Clacens, F. De Campo, A. Liebens, F. Dumeignil, M. Pera-Titus, Direct dehydration of 1,3-butanediol into butadiene over aluminosilicate catalysts, Catal. Sci. Technol. 6 (2016) 5830–5840. https://doi.org/10.1039/c5cy02211h.

[9] Y. Wang, D. Sun, Y. Yamada, S. Sato, Selective production of 1,3-butadiene in the dehydration of 1,4-butanediol over rare earth oxides, Appl. Catal. A Gen. 562 (2018) 11–18. https://doi.org/10.1016/j.apcata.2018.05.029.

[10] J.S. Kruger, T. Dong, G.T. Beckham, M.J. Biddy, Integrated conversion of 1-butanol to 1,3-

butadiene, RSC Adv. 8 (2018) 24068–24074. https://doi.org/10.1039/c8ra02977f.

[11] S. Akiyama, A. Miyaji, Y. Hayashi, M. Hiza, Y. Sekiguchi, T. ru Koyama, A. Shiga, T. Baba, Selective conversion of ethanol to 1,3-butadiene using germanium talc as catalyst, J. Catal. 359 (2018) 184–197. https://doi.org/10.1016/j.jcat.2018.01.001.

[12] A. Matsuda, Y. Matsumura, Y. Yamada, S. Sato, Vapor-phase dehydration of 1,4-butanediol to 1,3-butadiene over $Y_2Zr_2O_7$ catalyst, Mol. Catal. 514 (2021) 111853. https://doi.org/10.1016/j.mcat.2021.111853.

[13] O. Hakizimana, E. Matabaro, B.H. Lee, The current strategies and parameters for the enhanced microbial production of 2,3-butanediol, Biotechnol. Reports. 25 (2020) e00397. https://doi.org/10.1016/J.BTRE.2019.E00397.

[14] L. Zhang, Y. Yang, J. Sun, Y. Shen, D. Wei, J. Zhu, J. Chu, Microbial production of 2,3-butanediol by a mutagenized strain of Serratia marcescens H30, Bioresour. Technol. 101 (2010) 1961–1967. https://doi.org/10.1016/J.BIORTECH.2009.10.052.

[15] K. Petrov, P. Petrova, High production of 2,3-butanediol from glycerol by Klebsiella pneumoniae G31, Appl. Microbiol. Biotechnol. 84 (2009) 659–665. https://doi.org/10.1007/S00253-009-2004-X.

[16] M. Köpke, C. Mihalcea, F.M. Liew, J.H. Tizard, M.S. Ali, J.J. Conolly, B. Al-Sinawi, S.D. Simpson, 2,3-Butanediol production by acetogenic bacteria, an alternative route to chemical synthesis, using industrial waste gas, Appl. Environ. Microbiol. 77 (2011) 5467–5475. https://doi.org/10.1128/AEM.00355-11.

[17] M.E. Winfield, The catalytic dehydration of 2,3-butanediol to 1,3-butadiene, J. Counc. Sci. Ind. Res. 18 (1945) 412–423.

[18] D. Sun, Y. Li, C. Yang, Y. Su, Y. Yamada, S. Sato, Production of 1,3-butadiene from biomass-derived C4 alcohols, Fuel Process. Technol. 197 (2020) 106193. https://doi.org/10.1016/j.fuproc.2019.106193.

[19] H. Duan, Y. Yamada, S. Sato, Future prospect of the production of 1,3-butadiene from butanediols, Chem. Lett. 45 (2016) 1036–1047. https://doi.org/10.1246/CL.160595.

[20] W. Zhang, D. Yu, X. Ji, H. Huang, Efficient dehydration of bio-based 2,3-butanediol to butanone over boric acid modified HZSM-5 zeolites, Green Chem. 14 (2012) 3441–3450. https://doi.org/10.1039/C2GC36324K.

[21] J. Zhao, D. Yu, W. Zhang, Y. Hu, T. Jiang, J. Fu, H. Huang, Catalytic dehydration of 2,3-butanediol over P/HZSM-5: effect of catalyst, reaction temperature and reactant configuration on rearrangement products, RSC Adv. 6 (2016) 16988–16995. https://doi.org/10.1039/C5RA23251A.

[22] M.A. Nikitina, V.L. Sushkevich, I.I. Ivanova, Dehydration of 2,3-butanediol over zeolite catalysts, Pet. Chem. 56 (2016) 230–236. https://doi.org/10.1134/S0965544116030099.

[23] Q. Zheng, M.D. Wales, M.G. Heidlage, M. Rezac, H. Wang, S.H. Bossmann, K.L. Hohn, Conversion of 2,3-butanediol to butenes over bifunctional catalysts in a single reactor, J. Catal. 330 (2015) 222–237. https://doi.org/10.1016/j.jcat.2015.07.004.

[24] F. Zeng, W.J. Tenn, S.N.V.K. Aki, J. Xu, B. Liu, K.L. Hohn, Influence of basicity on 1,3-butadiene formation from catalytic 2,3-butanediol dehydration over γ-alumina, J. Catal. 344 (2016) 77–89. https://doi.org/10.1016/j.jcat.2016.09.003.

[25] H. Duan, M. Unno, Y. Yamada, S. Sato, Adsorptive interaction between 1,5-pentanediol and MgO-modified ZrO_2 catalyst in the vapor-phase dehydration to produce 4-penten-1-ol, Appl. Catal. A Gen. 546 (2017) 96–102. https://doi.org/10.1016/j.apcata.2017.07.048.

[26] H. Duan, D. Sun, Y. Yamada, S. Sato, Dehydration of 2,3-butanediol into 3-buten-2-ol catalyzed by ZrO_2, Catal. Commun. 48 (2014) 1–4. https://doi.org/10.1016/j.catcom.2014.01.018.

[27] H. Duan, Y. Yamada, S. Sato, Selective dehydration of 2,3-butanediol to 3-buten-2-ol over ZrO2 modified with CaO, Appl. Catal. A Gen. 487 (2014) 226–233. https://doi.org/10.1016/j.apcata.2014.09.007.

[28] H. Duan, Y. Yamada, S. Sato, Vapor-phase catalytic dehydration of 2,3-butanediol into 3-buten-2-ol over Sc_2O_3, Chem. Lett. 43 (2014) 1773–1775. https://doi.org/10.1246/cl.140662.

[29] U. Sanyal, A. Martinez, M. Guo, S. Subramaniam, M. Song, K.K. Ramasamy, Selective Dehydration of 2,3-Butanediol to 3-Buten-2-ol over In_2O_3Catalyst, Energy and Fuels. 35 (2021) 15742–15751. https://doi.org/10.1021/acs.energyfuels.1c01706.

[30] Q. Zheng, J. Grossardt, H. Almkhelfe, J. Xu, B.P. Grady, J.T. Douglas, P.B. Amama, K.L. Hohn, Study of mesoporous catalysts for conversion of 2,3-butanediol to butenes, J. Catal. 354 (2017) 182–196. https://doi.org/https://doi.org/10.1016/j.jcat.2017.08.017.

[31] H. Duan, Y. Yamada, S. Sato, Vapor-phase hydrogenation of acetoin and diacetyl into 2,3-butanediol over supported metal catalysts, Catal. Commun. 99 (2017) 53–56. https://doi.org/10.1016/j.catcom.2017.05.022.

[32] Q. Zheng, J. Xu, B. Liu, K.L. Hohn, Mechanistic study of the catalytic conversion of 2,3-butanediol to butenes, J. Catal. 360 (2018) 221–239. https://doi.org/10.1016/j.jcat.2018.01.034.

[33] K. Tanabe, Surface and catalytic properties of ZrO_2, Mater. Chem. Phys. 13 (1985) 347–364. https://doi.org/10.1016/0254-0584(85)90064-1.

[34] W. Li, H. Huang, H. Li, W. Zhang, H. Liu, Facile synthesis of pure monoclinic and tetragonal zirconia nanoparticles and their phase effects on the behavior of supported molybdena catalysts for methanol-selective oxidation, Langmuir. 24 (2008) 8358–8366. https://doi.org/10.1021/la800370r.

[35] M. Thommes, K. Kaneko, A. V. Neimark, J.P. Olivier, F. Rodriguez-Reinoso, J. Rouquerol, K.S.W. Sing, Physisorption of gases, with special reference to the evaluation of surface area and pore size distribution (IUPAC Technical Report), Pure Appl. Chem. 87 (2015) 1051–1069. https://doi.org/10.1515/pac-2014-1117.

[36] S. Brunauer, P.H. Emmett, E. Teller, Adsorption of gases in multimolecular layers, J. Am. Chem. Soc. 60 (1938) 309–319. https://doi.org/10.1021/JA01269A023.

[37] E.P. Barrett, L.G. Joyner, P.P. Halenda, The determination of pore volume and area distributions in porous substances. I. Computations from Nitrogen isotherms, J. Am. Chem. Soc. 73 (2002) 373–380. https://doi.org/10.1021/JA01145A126.

[38] Scherrer P., Nachr Ges Wiss Goettingen, Math. Phys. 2 (1918) 98–100. http://ci.nii.ac.jp/naid/20000745371/en/ (accessed July 26, 2021).

[39] J.M. Berty, Testing commercial catalysts in recycle reactors, Catal. Rev. 20 (1979) 75–96. https://doi.org/10.1080/03602457908065106.

[40] J.W. Thybaut, C.S. Laxmi Narasimhan, J.F. Denayer, G. V. Baron, P.A. Jacobs, J.A. Martens, G.B. Marin, Acid-metal balance of a hydrocracking catalyst: Ideal versus nonideal behavior, Ind. Eng. Chem. Res. 44 (2005) 5159–5169. https://doi.org/10.1021/ie049375.

[41] J.J. Carberry, The Catalytic Effectiveness Factor Under Nonisothermal Conditions, AIChE J. (1961) 350–351.

[42] C.D.P. P.B. Weisz, Interpretation of measurements in experimental catalysis, Adv. Catlaysis. 6 (1954) 143–196.

[43] D.E. Mears, Diagnostic criteria for heat transport limitations in fixed bed reactors, J. Catal. 20 (1971) 127–131. https://doi.org/10.1016/0021-9517(71)90073-X.

[44] S. Lowell, J.E. Shields, Adsorption isotherms, Powder Surf. Area Porosity. (1984) 11–13. https://doi.org/10.1007/978-94-009-5562-2_3.

[45] K.T. Jung, Y.G. Shul, A.T. Bell, The Preparation and Surface Characterization of Zirconia Polymorphs, Korean J. Chem. Eng. 18 (2001) 992–999. https://doi.org/10.1007/BF02705631.

[46] X. Liu, V. Fabos, S. Taylor, D.W. Knight, K. Whiston, G.J. Hutchings, One-step production of 1,3-butadiene from 2,3-butanediol dehydration, Chem. - A Eur. J. 22 (2016) 12290–12294. https://doi.org/10.1002/chem.201602390.

[47] Z. Al-Auda, H. Al-Atabi, K.L. Hohn, Metals on ZrO_2 : Catalysts for the aldol condensation of methyl ethyl ketone (MEK) to C8 ketones, Catalysts. 8 (2018) 1–15. https://doi.org/10.3390/catal8120622.

[48] M.A. Nikitina, I.I. Ivanova, Conversion of 2,3-butanediol over phosphate catalysts, ChemCatChem. 8 (2016) 1346–1353. https://doi.org/10.1002/cctc.201501399.

[49] H. Duan, Dehydration of 2 ,3-butanediol into 3-buten-2-ol and 1 ,3-butadiene over acid-base catalysts, (2017).

[50] C.D. Baertsch, K.T. Komala, Y.H. Chua, E. Iglesia, Genesis of Brønsted acid sites during dehydration of 2-butanol on tungsten oxide catalysts, J. Catal. 205 (2002) 44–57. https://doi.org/10.1006/jcat.2001.3426.

[51] X. Wang, R.Y. Saleh, U.S. Ozkan, Reaction network of aldehyde hydrogenation over sulfided Ni-Mo/Al_2O_3 catalysts, J. Catal. 231 (2005) 20–32. https://doi.org/10.1016/j.jcat.2004.12.010.

[52] H. Hattori, Basic catalysts and fine chemicals, Stud. Surf. Sci. Catal. 78 (1993) 35–49. https://doi.org/10.1016/S0167-2991(08)63302-9.

[53] F. Zeng, S.H. Bossmann, M.G. Heidlage, K.L. Hohn, Transformation of 2,3-butanediol in a dual bed catalyst system, Chem. Eng. Sci. 175 (2018) 387–395. https://doi.org/10.1016/j.ces.2017.10.009.

[54] G.S. Salvapati, K. V. Ramanamurty, M. Janardanarao, Selective catalytic self-condensation of acetone, J. Mol. Catal. 54 (1989) 9–30. https://doi.org/10.1016/0304-5102(89)80134-8.